Role of oxygen supply in high-temperature growth of compact oxide scale

DANIELE GOZZI, PIER LUIGI CIGNINI* LORENZO PETRUCCI
Dipartimento di Chimica, Università "La Sapienza", P. le Aldo Moro 5, 00185 Roma, Italy
MASSIMO TOMELLINI
Instituto di Chimica, Università della Basilicata, Potenza, Italy

High-temperature oxidation of metals at low oxygen impinging fluxes and low values of oxygen partial pressure were considered on the basis of the fundamental aspects of oxidation kinetics. To do this, the oxidation kinetics of copper to the monovalent oxide was studied under appropriate experimental conditions using apparatus consisting of two solid-state electrochemical cells, both with yttria stabilized zirconia as the solid electrolyte, coupled together. The cells operated as oxygen sensor and oxygen pump, respectively, in such a way that oxygen gas was generated and monitored very close to the surface of the oxidizing sample. The results obtained on copper foil at 1113 K over the oxygen pressure range 1×10^{-14} (highly purified argon) to 1500 Pa show a linear growth of the oxide for exposures up to 2000 sec. This was tentatively explained by assuming the oxygen supply to the sample surface to be the rate limiting step, instead of the solid state diffusion into the growing oxide.

1. Introduction

The growth of oxide films on metals has been the subject of many theoretical [1] and experimental [2, 3] studies and several models have been proposed to explain different trends of the kinetics of oxidation. In these models, the dependence of the kinetics of oxidation on experimental variables such as oxide thickness, gaseous phase composition, rate of interfacial reactions, temperature, etc., is considered through the characterization of the rate limiting step (RLS) of the overall oxidation process. This "choice" is given by the experimental growth conditions (including the oxide thickness) under which the oxidation is carried out.

As expected from the basic rules of experimental kinetics, a model of the oxidation kinetics is obtained through the identification and analytical description of the kinetics of the RLS. Depending on the oxide thickness and temperature, three different growth models can be considered: (1) initial stage of oxidation; (2) thin oxide films at low temperature; (3) thick oxide films at high temperatures. Obviously, these three cases do not exhaust the conditions under which an oxidation process can be realized.

As is well known [2, 3], the initial stage of oxidation of a clean metal surface is the gas adsorption over the metal itself. This process can be written as follows

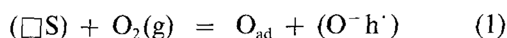

$$(\square S) + O_2(g) = O_{ad} + (O^- h^\cdot) \quad (1)$$

where $(\square S)$ is an adsorption site and $(O^- h^\cdot)$ a neutral pair consisting of an oxygen ion and a positive hole (Cu_2O for instance [4]). If the RLS of the oxidation is Process 1, the reaction rate will be proportional to the oxygen adsorption kinetics.

The formation of the thin oxide film (oxide thickness $\leqslant 5$ nm) at low temperature obeys Cabrera and Mott's theory [5] where the coupled current approach is used [6]. Owing to the low value of the oxide thickness, the RLS of the oxidation reaction is the ionic and electronic transport into the oxide film, where the electron transport is treated in terms of a quantum mechanics tunnel effect and reactions at the interfaces are considered to be fast. In this case, a logarithmic law of growth is expected and the oxygen activity does not influence the oxidation rate.

The growth of thick oxide films at high temperatures is treated by the Wagner's theory [7] where the RLS is the ionic and electronic transport into the oxide (ambipolar transport) described by the classical linear response theory. If the reactions at the interfaces are fast, a parabolic law of the oxide growth is expected in which the rate constant depends on the oxygen activity.

In the kinetic models mentioned before, the RLS only depends on the oxide properties: in the last two models, the transport properties have to be considered, whereas in the first model, it is the surface sticking coefficient, s. However, the oxygen supply to the sample surface could be rate-determining at low values of oxygen impinging flux. At a given temperature and oxygen partial pressure, P, the oxygen flux at

*Centro di Termodinamica Chimica alle Alte Temperature – CNR, c/o Dipartimento di Chimica, Universita "La Sapienza", P. le Aldo Moro 5, 00185 Roma, Italy.

0022–2461/90 $03.00 + .12 © 1990 Chapman and Hall Ltd.

the surface, J_k, is given by Knudsen's equation

$$J_k = sP/(2\pi mKT)^{1/2} \quad (2)$$

where m is the mass of the oxygen molecule. The equation is valid in equilibrium conditions.

Owing to the surface reaction, an oxygen concentration gradient could be established in the gaseous phase and an additional oxygen flux should be taken into account

$$J_D = -D\nabla C_0 \quad (3)$$

where C_0 is the concentration and D the diffusion coefficient of oxygen in the gas phase.

Therefore, in the oxidation of thick oxide films at high temperatures and low oxygen pressures, knowledge of $J_k(T, P)$, $J_D(T, P)$ and $J_W(T, P)$ fluxes, where, $J_W(T, P)$ is the oxidation flux predicted by Wagner, is important to characterize the RLS. If $J_W < J_k < J_D$ (or $J_W < J_D < J_k$), the RLS of the oxidation process is the ionic and electronic transport into the oxide film as mentioned before. If $J_k < J_W$ (with $J_k > J_D$) or $J_D < J_W$ (with $J_D > J_k$), the RLS is the supply of oxygen at the surface. This process does not depend on the oxide properties if the adsorption can be considered to be fast. In addition, it is important to point out that any theory considered should take into acount the thermodynamic requirements for the feasability of the oxidation reaction. In fact, in Wagner's theory, the equation of the rate constant is

$$k_W(P, T) = A(T)\,[(P^{\pm 1/n} - P_O^{\pm 1/n})] \quad (4)$$

where "$\pm$" refers, respectively, to p-type and n-type semiconductor oxide, n is an integer and P_O the oxygen pressure in the equilibrium of oxide formation. The reaction rate is

$$J_W(P, T) = k_W(P, T)/x \quad (5)$$

where x is the oxide thickness. To have $J_W(P, T) > 0$, the inequality $P > P_O$ must be satisfied. This is a sufficient requirement, under Wagner's hypothesis, for the oxidation reaction.

Generally, oxidation experiments are carried out in a furnace under gas flux [8]. In steady-state conditions, the average oxygen pressure can be low and the gas impinging flux, J_i, sufficiently high to fulfil the inequality $J_i > J_W$ in such a way that the oxide grows with a parabolic law. If the inequality is reversed, this kind of growth cannot be realized.

Some years ago our laboratory undertook a programme of study of the kinetics of the reaction at high temperatures and low oxygen partial pressures between oxygen and materials. Until now, particular attention was paid to metals [9–15]. The scope of the present work is to study the oxidation kinetics of a metal when the above inequalities are taken into consideration. This was realized by using a particular experimental arrangement [15] which allows production of tunable oxygen fluxes and detection of the oxygen partial pressure, both in proximity to the sample surface. Copper was chosen as the test sample.

2. Experimental procedure

A detailed description of the electrochemical apparatus is reported elsewhere [15]; further details are given below.

Two yttria-stabilized zirconia (YSZ) tubes are assembled in such a way as to create, at the flat ends, the housing for an alumina microchamber where the sample under study is placed. The innermost YSZ tube (7 wt % Y_2O_3, F.E.R, Milan, Italy) is the oxygen sensor and the other is the oxygen pump (8 wt % Y_2O_3, Zircoa Co., USA). Porous platinum electrodes were obtained by covering both sides of the YSZ tube flat ends with platinum paste according to the standard procedure.

A flux of high-purity argon (HPA) is allowed to circulate through holes in the microchamber for washing purposes. Using a home-made purification system, HPA is produced and continuously monitored by an on-line YSZ oxygen sensor [12]. The oxygen partial pressure in the HPA stream was normally maintained at 1×10^{-14} Pa with a flow rate of 27.5 scm min^{-1} controlled by a Matheson (USA) transducer. When the pump was oxygen producing, the HPA stream was stopped and measurements were carried out in a static atmosphere.

The cell assembly was placed in a horizontal high-vacuum alumina furnace. All the leads were of platinum wire up to the cold zone of the furnace.

A digital differential electrometer (Amel 631, Italy) was used to measure the oxygen sensor e.m.f. and a set of instruments was interconnected, composed of a potentiostat/galvanostat (Amel 551), an analogue function generator (Amel 566), and a digital integrator (Amel 731) was used to drive the oxygen pump polarizations. Measurements were taken using an automatic data aquisition system.

No particular treatment was done to the samples. They were cut to the appropriate dimensions and cleaned in an ultrasonic bath with a non-aqueous detergent. The purity of the samples was better than 99.9%. Samples were placed either vertically with one side in front of the pump and the other side in front of the oxygen sensor, or horizontally in a thin BN holder.

All the results shown refer to experiments carried out at 1113 K on copper samples shaped as laminae of 14 mm × 5 mm × 1 mm thick and at a nominal 10 mA cm^{-2} current density applied to the oxygen pump. The outer and inner atmosphere of the pump and sensor was pure oxygen at atmospheric pressure, P_r.

3. Results and discussion

Fig. 1 shows the e.m.f. response of the oxygen sensor in different experimental arrangements of the sample in the microchamber [15]. Curve B is the e.m.f., E, recording without sample in the microchamber and the other curves are recordings with the samples. We found that the sample position with respect to the ideal line joining sensor and pump (LJSP), affected the oxygen consumption. In the perpendicular double side (PDS) curve, the sample was placed perpendicular to LJSP with both sides parallel to the pump and sensor planes and in the parallel one side (POS) curve only one side, parallel to LJSP, is exposed to the gaseous phase.

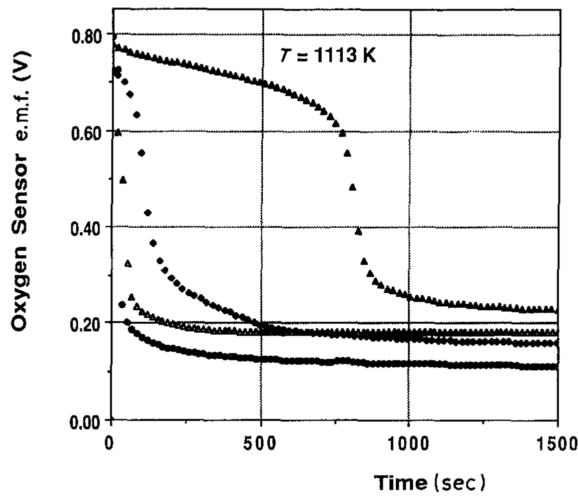

Figure 1 E.m.f. recordings of the oxygen sensors as obtained in the oxidation of a copper sample placed in different positions in the microchamber. (▲) BNP: sample perpendicular to LJSP with the side facing the pump covered by BN paste. (◆) POS: sample parallel to LJSP, only one side exposed to the gas phase. (△) PDS: sample perpendicular to LJSP with one side facing the pump and the other facing the sensor. (●) B: control (without sample).

Fig. 2 is derived from Fig. 1 in which each curve is converted into oxygen partial pressure, $P(t)$, by the well-known equation

$$P(t) = P_r \exp(-4FE/RT) \quad (6)$$

An explanation of the different trends of the curves was given elsewhere [15]. Here we are interested in finding the correct meaning of P as read by the sensor, because this quantity will be fundamental to the next considerations. In the PDS position, the probability, Z, that an oxygen molecule reaches the oxygen sensor is given by

$$Z = Z_1 \times Z_2 \quad (7)$$

where Z_1 is the probability that an oxygen molecule gets over the shielding-sensor sample and reaches the sensor, and Z_2 is the probability that an oxygen molecule is captured from the sample surface. Both probabilities are assumed independent. Z_1 depends on geometrical terms according to the equation

$$Z_1 = (A_{mc} - A_s \sin\theta)/A_{mc} \quad (8)$$

where A_{mc}, A_s and θ are, respectively, the cross-sectional area of the microchamber, the surface area of the sample and the angle between the plane of the sample and the LJSP. Z_2 depends on the oxygen concentration gradient which is established at the sample surface, this being related to the physical and chemical reactivity of the sample surface itself.

The boron nitride perpendicular (BNP) curve, in which the sample is again placed perpendicular to LJSP, but with the side facing the oxygen pump made unreactive by a layer of BN paste, shows the response of the sensor when the causes giving rise to Z_2 are removed.

In the POS case, $\theta = 0$, $Z_1 = 1$ and $Z_2 \neq 0$. This condition does not differ at all from the control Curve B, therefore, we can assume that the oxygen partial pressure at the sensor surface is practically the same as the pump surface. Consequently, the oxygen partial pressure read by the sensor can be reasonably assumed to be the average oxygen partial pressure in the microchamber. Owing to the reactivity of the sample, the oxygen partial pressure at its surface will be significantly lower than that in the bulk of the microchamber and the oxygen concentration gradient can be considered localized in a very narrow region around the sample.

Fig. 3 shows the curves of the calculated and experimental oxygen fluxes plotted against time, supplied to the sample surface. The oxygen partial pressure data of the POS curve of Fig. 2 were used throughout in the respective calculations. J_k was calculated using Equation 2 and the J_W fluxes from Equation 5, inserting in it the literature data of the rate constant of high-temperature oxidation of copper to Cu_2O. We selected the data of Baur *et al.* [16] and Tomlinson and Yates [17] because of the closeness to our experimental conditions. Therefore, we have, respectively,

$$J_W [16] = (2.5 \times 10^{-6}) [(P^{1/4}(t) - P_O^{1/4})/t]^{1/2} \quad (9)$$

and

$$J_W [17] = (1.4 \times 10^{-5}) [(P^{1/4}(t) - P_O^{1/4})/t]^{1/2} \quad (10)$$

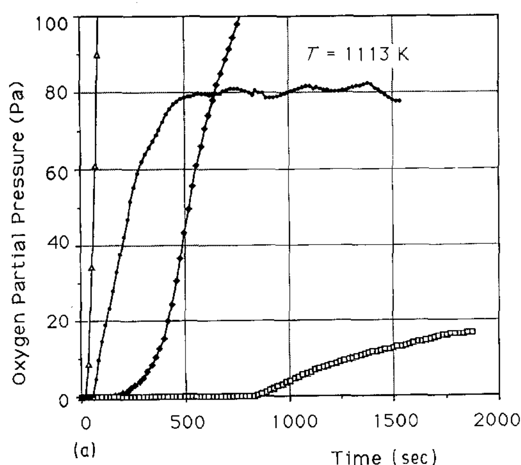

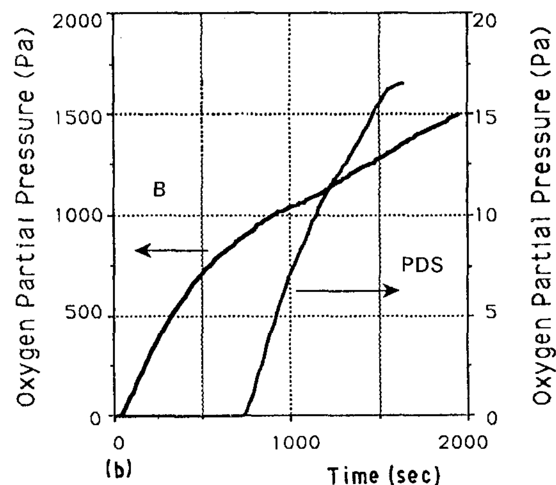

Figure 2 (a) Oxygen partial pressure trends in the microchamber calculated from the curves of Figs 1 through Equation 5. (△) B, (◆) POS, (□) PDS, (●) BNP. (b) The complete trends for the B and PDS curves.

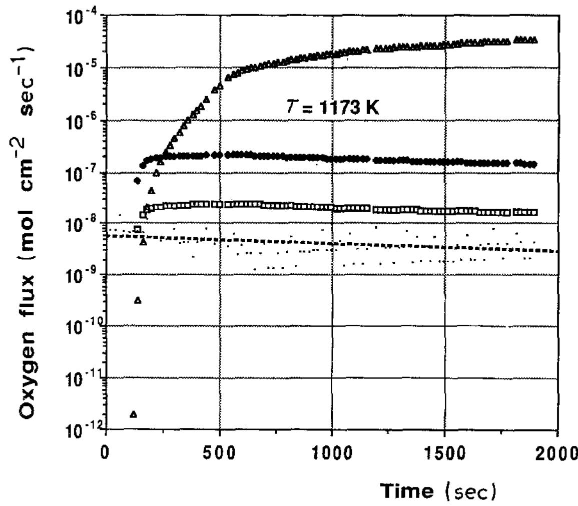

Figure 3 Trends of the oxygen fluxes for copper oxidation both as found and calculated using literature and POS (Fig. 2) pressure data. (□) J_W [16], (△) J_k, (◆) J_W [17], (- - -) J_{exp}.

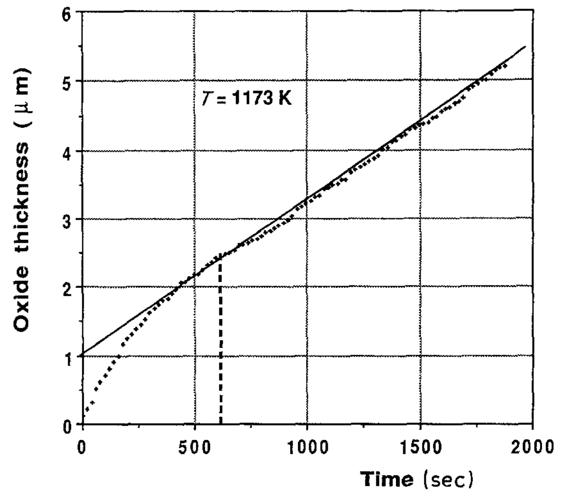

Figure 4 Kinetics of the Cu_2O growth on copper. The best fit to the straight line of the linear tract is given by Equation 12.

where P_O at 1113 K is equal to 4.58×10^{-6} Pa for the $Cu(s)/Cu_2O(s)$ equilibrium [18].

J_{exp} was calculated by applying the oxygen mass balance in the microchamber through the continuity equation

$$\int_{V_{mc}} \frac{\partial C_O}{\partial t} \mathrm{d}v = \int_S (\Sigma_i \boldsymbol{J}_i) \, \mathrm{d}\boldsymbol{\sigma} \quad (11)$$

where $\boldsymbol{J}_i$ is the ith flux and the integral on the right-hand side is calculated on the internal surface of the microchamber. If all the $\boldsymbol{J}_i$ are considered perpendicular to the respective surface elements, $\mathrm{d}\sigma_i$, Equation 11 becomes

$$\int \frac{\partial C_0}{\partial t} \mathrm{d}v = \frac{\partial}{\partial t} \int C_0 \mathrm{d}v$$

$$= V_{mc} \frac{\partial}{\partial t} \frac{1}{V_{mc}} \int C_0 \mathrm{d}v = V_{mc} \frac{\mathrm{d}\bar{C}_0}{\mathrm{d}t} = \Sigma J_i S_i \quad (12)$$

where $\bar{C}_0 = P(t)/RT$ is the average oxygen concentration in the volume, V_{mc}, being $P(t)$ the average oxygen partial pressure in the microchamber. In addition, J_{exp} was calculated by taking into account the control Curve B [15]. All fluxes are given in mol O_2 cm^{-2} sec^{-1}.

The trend in the thickness, x, of Cu_2O growth, obtained as the difference between the B and PDS curves of Fig. 2 multiplied by $V_m/2$, where V_m is the oxide molar volume, is reported in Fig. 4. After a time, which was about the 30% of the length of the experiment the oxide began to grow linearly. The regression line calculated on many experimental points along that tract was

$$x(\mu m) = 1.01 + 2.23 \times 10^{-3} t\,(s) \quad (13)$$

with a correlation factor equal to 0.9999.

Now, some considerations can be made.

1. As reported in Fig. 3, the oxygen flux experimentally consumed by the sample is lower than all the other fluxes, although between those calculated from the literature data, there is a difference of an order of magnitude. If the Wagner mechanism is still considered, this implies that the oxygen activity at the sample surface is lower than the oxygen activity in the gas phase. At constant temperature, k_W only depends on the oxygen activity because in the Wagner's theory no other processes are considered at the oxide/gas phase interface. On the other hand, as mentioned before, the oxygen activity on the sample surface could be lower.

2. The linear growth (Fig. 4) disagrees with the Wagner's parabolic growth and better matches a different RLS, exhibiting a constant reaction rate. This RLS could be the adsorption of oxygen in which, the oxygen surface coverage at the equilibrium can be expressed by Langmuir's equation. As usual, if the oxygen activity in the gas phase is very low, the equilibrium surface coverage is proportional to this quantity itself. On this basis, the kinetic and thermodynamic quantities of the adsorption process are given by

$$J_a = s(\theta_s) J_s \quad (14)$$

$$\theta_s = K_a\, a/(1 + K_a a) \quad (15)$$

where J_a, J_s, θ_s, K_a and a are, respectively, the adsorption flux, the impinging flux, the surface coverage, Langmuir constant and the oxygen gas activity at the surface. Because the sticking coefficient is a function of the surface coverage, at J_s constant with time, J_a is still a function of time. In a reactive surface, as in an oxidation process, the change of the surface coverage is also a function of the surface reactivity. If the rate of the surface oxygen conversion to oxide is higher than J_s, the surface coverage will be approximately zero and the sticking coefficient practically unity. Therefore, J_a, will be the rate of overall oxidation process and it will be constant with time, therefore the thickness growth rate will be constant according to

$$\mathrm{d}x/\mathrm{d}t = (V_m/2)\, J_a \quad (16)$$

In the past, the problem of oxygen activity at an oxidizing surface considered in the framework of Wagner's theory was treated by Baur *et al.* [16], who considered the oxygen adsorption at the Cu_2O surface to be much faster than the solid state diffusion within

the oxide, because their findings were in agreement with a parabolic law.

4. Conclusions

Some aspects of the high-temperature oxidation of metals have been discussed on the basis of a fundamental approach to the mechanism of this process. In particular, we refer to low oxygen partial pressure conditions because of the growing interest in technological applications of metals, alloys and intermetallics under those experimental conditions.

A specific experimental arrangement shows the potential to oxidize metals at low oxygen fluxes impinging their surfaces and low values of oxygen partial pressure. Under these conditions, the results obtained did not show clearly that the solid state diffusion into the growing oxide is the RLS of the overall oxidation process, because a linear growth rate on copper was found. Therefore, we can tentatively conclude that the RLS is the oxygen supply to the reactive surface.

Acknowledgements

This work was carried out with partial financial support of the Centro di Termodinamica Chimica alle Alte Temperature of the National Research Council. The co-operation of Dr D. Ferro for the SEM analysis, as well as the contribution of technician Mr S. Simonetti who made some mechanical parts of the experimental apparatus, are also acknowledged.

References

1. A. T. FROMHOLD Jr, in "Theory of Metal Oxidation", Vol. I, Defects in Crystalline Solids Series, edited by S. Amelincks, R. Gevers and J. Nihoul (North-Holland, Amsterdam 1976) p. 69.
2. PER KOFSTAD, "High Temperature Oxidation of Metals" (Wiley, New York, 1966).
3. *Idem*, "High Temperature Corrosion" (Elsevier, London, 1988).
4. J. E. BOGGIO, *J. Chem. Phys.* **53** (1970) 3544.
5. N. CABRERA and N. F. MOTT, *Rep. Progr. Phys.* **12** (1949) 163.
6. A. T. FROMHOLD Jr and E. L. COOK, *Phys. Rev. Lett B* **17** (1966) 1212.
7. C. WAGNER, *Z. Phys. Chem.* **B21** (1933) 25.
8. E. T. TURKDOGAN, W. M. McKEWAN and L. ZWELL, *J. Chem. Phys.* **60** (1965) 327.
9. D. GOZZI *Mater. Chem. Phys.* **8** (1983) 503.
10. *Idem, Solid State Ionics* **14** (1984) 239.
11. D. GOZZI and G. De MARIA, *High Temp. Sci.* **22** (1986) 27.
12. M. TOMELLINI and D. GOZZI, *Oxid. Metals* **26** (1986) 305.
13. M. TOMELLINI, D. GOZZI, A. BIANCONI and I. DAVOLI, *J. C. S. Faraday Trans., I* **83** (1987) 289.
14. D. GOZZI, M. TOMELLINI, P. L. CIGNINI and L. PETRUCCI, *J. Electrochem. Soc.* **134** (1987) 728.
15. D. GOZZI, P. L. CIGNINI, G. CARNEVALE, L. PETRUCCI and M. TOMELLINI, *High Temp. High Press.* **20** (1988) 385.
16. J. P. BAUR, D. W. BRIDGES and W. M. FASSEL Jr, *J. Electrochem. Soc.* **103** (1956) 273.
17. W. J. TOMLINSON and J. YATES, *J. Phys. Chem. Solids* **38** (1977) 1205.
18. JANAF Thermochemical Tables (NSRDS-NBS 37, 1971) and Supplement 1974, *J. Phys. Chem. Ref.* Data (1974) 463.

Received 21 April
and accepted 16 August 1989